Methods

Nogo recombinant proteins

To express Amino-Nogo, the human Nogo-A cDNA for residues 1–1,040 was ligated into pcDNA3.1MycHis (Invitrogen, Burlingame, California) with an in-frame Myc-His tag. We transfected this plasmid into HEK293T cells and Amino-Nogo was purified with a Ni^{2+} resin[10]. The human Nogo-66 sequence was ligated into pcAP-5 (ref. 10) in frame with the signal sequence, 6×His tag and placental AP coding region. This plasmid was transfected into HEK293 cells, and secreted AP–Nogo was purified by Ni^{2+} affinity chromatography. GST–Nogo-66 has been described[1].

Nogo-66 receptor binding assays and expression cloning

To detect AP–Nogo binding, cultures were washed with Hanks balanced salt solution containing 20 mM sodium HEPES, pH 7.05, and 1 mg ml^{-1} bovine serum albumin (BSA) (HBH). The plates were then incubated with AP–Nogo in HBH for 2 h at 23 °C. We detected and quantified bound AP–Nogo as for AP–Sema3A[11]. For saturation analysis of AP–Nogo bound to COS-7 cells, bound AP–Nogo protein was eluted with 1% Triton X-100. After heat inactivation of endogenous AP, we measured AP–Nogo using *p*-nitrophenyl phosphate as substrate.

For expression cloning of a Nogo-66 receptor, pools of 5,000 arrayed clones from a mouse adult-brain cDNA library (Origene Technologies, Rockville, Maryland) were transfected into COS-7 cells, and AP–Nogo binding was assessed. We isolated single NgR cDNA clones by sib selection and sequenced them. A Myc–NgR vector was created in pSecTag2-Hygro (Invitrogen) using the signal peptide of pSecTag2 fused to Myc and residues 27–473 of NgR. Human NgR cDNA was predicted from a human genomic cosmid sequence (AC007663). Oligonucleotide primers based on the predicted human cDNA amplified the cDNA from a human adult-brain cDNA library (Origene Technologies).

To assess binding of Myc–NgR to the cell membrane, particulate fractions were treated with or without 5 U PI-PLC (Sigma, St. Louis, MO) per mg of HEK293T cell protein for 1 h at 30 °C in HBH. After centrifugation at 100,000*g* for 1 h, we analysed equal proportions of the soluble and particulate fractions. To assess the physical interaction of NgR with Nogo-66, we incubated the PI-PLC extract (50 μg total protein) with 10 μg GST–Nogo-66 or buffer, or 10 μg GST for 1 h at 23 °C. We added glutathione-coupled agarose to bind GST and associated proteins. We analysed bound proteins by anti-Myc immunoblot.

RNA analysis

For northern blots, 1 μg poly(A)$^+$ RNA from each adult mouse tissue on a nylon membrane (Origene Technologies) was hybridized with a full-length ^{32}P-labelled probe[1,12]. We used digoxegenin-labelled riboprobes (nucleotides 1–1,222) and adult mouse brain sections[1,12] for *in situ* hybridization. The sense probe produced no signal.

Nogo-66 receptor antibodies

A GST–NgR (residues 27–447) fusion protein was purified from *Escherichia coli* and used to immunize rabbits. We diluted immune serum 3,000-fold for immunoblots and 1,000-fold for immunohistology on tissue-culture samples that had been fixed by formalin. Staining of tissue was totally abolished by addition of 5 μg ml^{-1} GST–NgR.

Cell spreading, neurite outgrowth and viral infection

To measure spreading rates, subconfluent NIH 3T3 fibroblasts or COS-7 cells were plated for 1 h in serum-containing medium before fixation and staining with rhodamine-phalloidin. Glass coverslips were precoated with 100 μg ml^{-1} poly-L-lysine, washed, and then 3 μl drops of PBS containing 15 pmol Amino-Nogo, 15 pmol GST–Nogo-66, 15 pmol poly-Asp (M_r 35 K, Sigma), or no protein were spotted and dried. We added soluble Nogo protein preparations (100 nM) at the time of plating. Amino-Nogo was added alone or after a pre-incubation with a twofold molar excess of anti-Myc 9E10 antibody, or with a twofold excess of anti-Myc plus a twofold excess of purified goat anti-mouse IgG.

Chick E5 spinal cord, chick E7–E13 DRG, chick E7 retina and mouse P4 cerebellar neuron culture, growth-cone-collapse assays and neurite-outgrowth assays have been described[1,10–13]. Here, outgrowth from dissociated neurons was assessed after 12–24 h. For the substrate-bound experiments, glass chamber slides were coated with 100 μg ml^{-1} poly-L-lysine, washed, and then 3 μl drops of PBS containing 15 pmol Amino-Nogo, 15 pmol GST–Nogo-66, 15 pmol poly-Asp, or no protein were spotted and dried. After three PBS washes, we coated slides with 10 μg ml^{-1} laminin. After aspiration of laminin, dissociated neurons were added. For the soluble Nogo experiments, slides were coated with poly-L-lysine and laminin in the same fashion, and then 100 nM Amino-Nogo, 100 nM clustered Amino-Nogo, or 100 nM GST–Nogo-66 was added to the culture medium at the time of plating. After 1 d *in vitro*, some DRG explants were treated for 30 min with 1 unit ml^{-1} PI-PLC (Sigma) before the growth-cone-collapse assay.

An HSV-Myc–NgR stock was prepared as described[10]. We infected E7 retinal explants for 24 h. We stained some cultures infected with HSV-Myc–NgR with anti-Myc antibody to verify protein expression. Error bars reflect the s.e.m. from 4–8 determinations.

Received 3 July; accepted 30 October 2000.

1. GrandPre, T., Nakamura, F., Vartanian, T. & Strittmatter, S. M. Identification of the Nogo inhibitor of axon regeneration as a reticulon protein. *Nature* **403,** 439–444 (2000).
2. Chen, M. S. *et al.* Nogo-A is a myelin-associated neurite outgrowth inhibitor and an antigen for monoclonal antibody IN-1. *Nature* **403,** 434–439 (2000).
3. Prinjha, R. *et al.* Inhibitor of neurite outgrowth in humans. *Nature* **403,** 383–384 (2000).
4. Schwab, M. & Caroni, P. Oligodendrocytes and CNS myelin are non-permissive substrates for neurite growth and fibroblast spreading *in vitro*. *J. Neurosci.* **8,** 2381–2393 (1988).
5. Caroni, P. & Schwab, M. E. Two membrane protein fractions from rat central myelin with inhibitory properties for neurite growth and fibroblast spreading. *J. Cell Biol.* **106,** 1281–1288 (1988).
6. Flanagan, J. G. & Leder, P. The kit ligand: a cell surface molecule altered in steel mutant fibroblasts. *Cell* **63,** 185–194 (1990).
7. Schnell, L. & Schwab, M. E. Axonal regeneration in the rat spinal cord produced by an antibody against myelin-associated neurite growth inhibitors. *Nature* **343,** 269–272 (1990).
8. Buffo, A. *et al.* Application of neutralizing antibodies against NI-35/250 myelin-associated neurite growth inhibitory proteins to the adult rat cerebellum induces sprouting of uninjured Purkinje cell axons. *J. Neurosci.* **20,** 2275–2286 (2000).
9. Thallmair, M. *et al.* Neurite growth inhibitors restrict plasticity and functional recovery following corticospinal tract lesions. *Nature Neurosci.* **1,** 124–131 (1998).
10. Nakamura, F., Tanaka, M., Takahashi, T., Kalb, R. G. & Strittmatter, S. M. Neuropilin-1 extracellular domains mediate semaphorin D/III-induced growth cone collapse. *Neuron* **21,** 1093–1100 (1998).
11. Takahashi, T., Nakamura, F., Jin, Z., Kalb, R. G. & Strittmatter, S. M. Semaphorins A and E act as antagonists of neuropilin-1 and agonists of neuropilin-2 receptors. *Nature Neurosci.* **1,** 487–493 (1998).
12. Goshima, Y., Nakamura, F., Strittmatter, P. & Strittmatter, S. M. Collapsin-induced growth cone collapse mediated by an intracellular protein related to UNC-33. *Nature* **376,** 509–514 (1995).
13. Huang, D. W., McKerracher, L., Braun, P. E. & David, S. A therapeutic vaccine approach to stimulate axon regeneration in the adult mammalian spinal cord. *Neuron* **24,** 639–647 (1999).

Acknowledgements

This work was supported by grants to S.M.S. from the NIH and the Christopher Reeve Paralysis Foundation. A.F. was an FCAR research fellow. S.M.S. is an Investigator of the Patrick and Catherine Weldon Donaghue Medical Research Foundation.

Correspondence and requests for materials should be addressed to S.M.S. (e-mail: stephen.strittmatter@yale.edu). The mouse and human Nogo-66 receptor mRNA sequences are deposited in GenBank under accession numbers AF283462 and AF283463, respectively.

Maize *yellow stripe1* encodes a membrane protein directly involved in Fe(III) uptake

Catherine Curie*†, Zivile Panaviene†‡, Clarisse Loulergue*, Stephen L. Dellaporta§, Jean-Francois Briat* & Elsbeth L. Walker‡

** Biochimie et Physiologie Moléculaire des Plantes, Centre National de la Recherche Scientifique (Unité Mixte de Recherche 5004), Institut National de la Recherche Agronomique, Université Montpellier 2 et École Nationale Supérieure d'Agronomie, Place Viala, F-34060 Montpellier cedex 1, France*
‡ Biology Department, University of Massachusetts, Amherst, Massachusetts 01003, USA
§ Molecular, Cellular & Developmental Biology Department, Yale University, New Haven, Connecticut 06520-8104, USA
† These authors contributed equally to this work

Frequently, crop plants do not take up adequate amounts of iron from the soil, leading to chlorosis, poor yield and decreased nutritional quality. Extremely limited soil bioavailability of iron has led plants to evolve two distinct uptake strategies: chelation, which is used by the world's principal grain crops[1,2]; and reduction, which is used by other plant groups[3–5]. The chelation strategy involves extrusion of low-molecular-mass secondary amino acids (mugineic acids) known as 'phytosiderophores', which chelate sparingly soluble iron[6]. The Fe(III)-phytosiderophore complex is then taken up by an unknown transporter at the root surface[7,8]. The maize *yellow stripe1* (*ys1*) mutant is deficient in Fe(III)-phytosiderophore uptake[7–10], therefore YS1 has been suggested to be the Fe(III)-phytosiderophore transporter. Here we show that *ys1* is a membrane protein that mediates iron uptake. Expression of YS1 in a yeast iron uptake mutant restores growth specifically on Fe(III)-phytosiderophore media. Under iron-deficient conditions, *ys1* messenger RNA levels increase in both roots and shoots.

Cloning of *ys1* is an important step in understanding iron uptake in grasses, and has implications for mechanisms controlling iron homeostasis in all plants.

We isolated a family that segregated ~25% of yellow striped mutants (Fig. 1a) in a random *Ac* transposon mutagenesis population[11]. Genomic blotting using *Ac* as a probe confirmed co-segregation of an *Ac*-containing *Sal*I restriction fragment of 9.5 kilobases (kb) with the yellow striped mutant phenotype in this family (Fig. 1b). Complementation assays (data not shown) were performed with the new yellow stripe mutation to show that it is allelic to *ys1*, and so is designated *ys1-m1::Ac*. Linkage of *ys1-m1::Ac* and *pr1* on chromosome 5 was tested (see Methods), and confirmed that the new mutation is linked to *pr1*.

We prepared a genomic library from the DNA of a mutant plant, and a clone containing the co-segregating 9.5-kb *Sal*I insert was identified using *Ac* sequences as a probe (Fig. 1d). A flanking probe containing sequences adjacent to the *Ac* element (YS1-XX; see Fig. 1d) was prepared and used on a second genomic blot of the original family segregating for the yellow stripe mutation (Fig. 1b). Each mutant individual contained the 9.5-kb *Sal*I fragment, as did heterozygous wild-type plants. One mutant plant contained a 5.2-kb *Sal*I fragment, which is the expected size of a fragment after transposition of *Ac* from the 9.5-kb fragment. Notably, neither heterozygous nor homozygous wild-type plants showed the expected 5.2-kb *Sal*I fragment. The lack of the 5.2-kb fragment is probably due to cytosine methylation of the *Sal*I sites in the wild-type *Ys1* allele. To confirm the co-segregation analysis, we prepared DNA from a second family that segregated the yellow stripe mutation, so that co-segregation in a new set of individuals could be tested. The DNA was digested with *Eco*RV, an enzyme that is insensitive to methylation (Fig. 1c). On these blots, the smaller fragment (lacking *Ac*) co-segregated with the wild-type phenotype, as expected.

The YS1-XX probe was used to screen a complementary DNA library prepared from roots of iron-deficient maize plants[12]. Three full-length or nearly full-length *ys1* cDNAs were recovered. Although the precise sizes of the three cDNAs differed because of alternative polyadenylation sites and sizes of 5′ untranslated regions (UTRs), they all encoded identical proteins. The sequence of these cDNAs indicates that the YS1 protein is 682 amino-acids long and contains 12 putative transmembrane domains (Fig. 2a), thus YS1 is likely to be localized to a membrane and has a structure consistent with its being a transporter protein.

The amino-acid sequence predicted from the *ys1* cDNA does not show strong similarity to any protein of known function in the various sequence databases, but it does show strong similarity to many expressed sequence tag (EST) clones in diverse plant species including both monocots and dicots, gymnosperms and mosses. The amino-acid sequence of YS1 also shows strong, full-length similarity to eight predicted *Arabidopsis* proteins (which we have designated YELLOW STRIPE1-LIKE (YSL) 1–8) of unknown function: YSL1 (491/665 residues 73% similarity; GenBank accession no. ATAC002343; PID no. AAB63613.1), YSL2 (511/658 residues 77% similarity; GenBank accession no. AB016884), YSL3 (516/668 residues 76% similarity; GenBank accession no. AB015476), YSL4 (452/644 residues 69% similarity; GenBank accession no. AB010072), YSL5 (460/680 residues 67% similarity; GenBank accession no. AB022219), YSL6 (430/604 residues 70% similarity; GenBank accession no. AB026649), YSL7 (472/674 residues 69% similarity; GenBank accession no. AC007234), and YSL8 (454/672 residues 67% similarity; GenBank accession no. AC007932; PID no. AAD49762.1).

YS1 also belongs to a gene family in maize, as there are three related maize ESTs present in GenBank. YS1 shows weak but significant similarity to a hypothetical yeast protein, YGL114 (36% similarity), belonging to the major facilitator superfamily (MFS; reviewed in ref. 13), which includes single-polypeptide secondary carriers that typically transport small solutes in response to chemiosmotic ion gradients, and to the *EspB* gene of *Myxococcus xanthus* (39% similarity). Notably, the 50 amino-terminal amino acids of YS1 contain 48% of the glutamic-acid residues of the protein (11/23). Some of these are in the sequence REKELELELER,

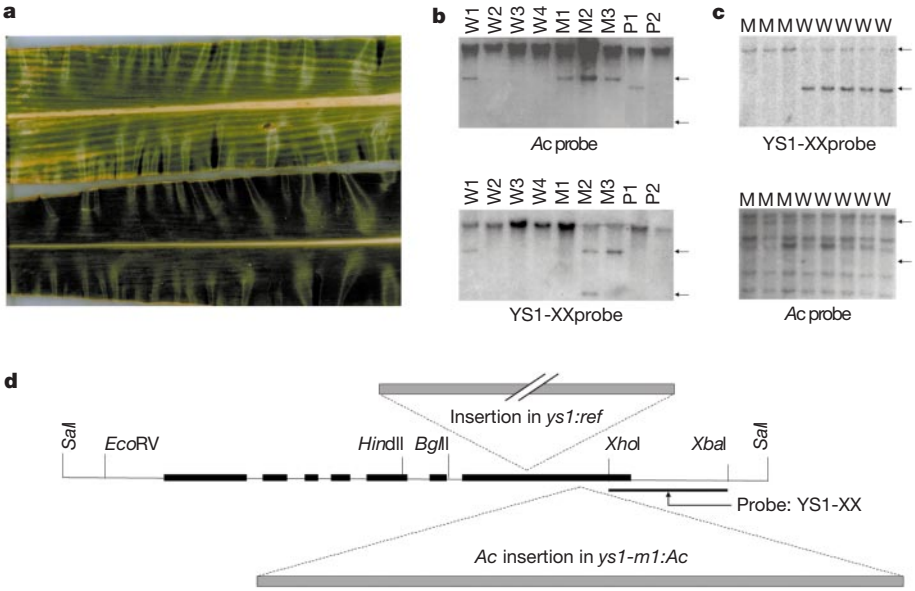

Figure 1 The *Ac*-induced yellow stripe mutation. **a**, Phenotype of homozygous mutant (above) and wild-type (below) maize leaves. **b**, Genomic blots of individuals from the original family segregating phenotypically wild-type (W1–W5) and mutant (M1–M3) individuals. DNA from the parental strains, *P-VV* (P1; the *Ac*-donor locus) and *r-m3* (P2) are also shown. All samples were digested with the restriction enzyme *Sal*I. The *Ac* probe was the internal *Hin*dIII fragment of *Ac*. The YS1-XX probe is indicated in **d**. Arrows indicate the positions of the fragments hybridizing to the YS1-XX probe. **c**, Genomic blot analysis of individuals from a second family segregating phenotypically wild-type (W) and mutant (M) individuals. All samples were digested with the restriction enzyme *Eco*RV. The blot was first probed with YS1-XX (above), and was then stripped and re-probed with the *Ac* probe (below). Arrows indicate the positions of the fragments hybridizing to the YS1-XX probe. **d**, Map of the *ys1* gene. Exons are indicated by black boxes. The positions of the *Ac* element in the *ys1-m1::Ac* allele and the retrotransposon element in the *ys1:ref* allele are indicated above and below. The probe fragment YS1-XX is also shown.

which is reminiscent of the REGLE sequence involved in Fe(III) transport[14]. This abundance of glutamic-acid residues at the amino terminus is conserved among six of the eight *Arabidopsis* YSL orthologues (data not shown).

We determined the sequence of the *ys1-m1::Ac* genomic clone λYS31. *Ac* is inserted in the coding region at amino-acid position 649 relative to the presumed start of translation (Fig. 2b). The *Ys1* wild-type and *ys1-ref* alleles were amplified from genomic DNA using primers selected on the basis of the cDNA sequence. Genomic blot analysis (data not shown) combined with polymerase chain reaction (PCR) of the corresponding genomic region indicates that the *ys1-ref* allele has a large insertion at amino-acid position 472 relative to the start of translation (Fig. 2b). Analysis of the ends of the inserted sequence indicates that it is a long-terminal repeat retrotransposon (data not shown). Two additional *ys1* mutant alleles, *ys1:74-1924-1* and *ys1:5344*, were amplified and sequenced (Fig. 2c). The *ys1:74-1924-1* mutation corresponds to a single nucleotide insertion that causes a frameshift altering the carboxy-terminal third of the protein sequence. The *ys1:5344* allele has a slightly more complicated mutation involving a 16-base-pair (bp) deletion accompanied by a 2-bp insertion that causes a frameshift starting in the last transmembrane domain of the protein. The sequence disruption in these additional *ys1* mutant alleles provides the final confirmation that we have cloned the *ys1* gene.

Saccharomyces cerevisiae double mutant *fet3fet4* (strain DEY1453) is defective in both low- and high-affinity iron(II) uptake systems, cannot grow on iron-limited medium[3], and cannot use iron complexed with the maize phytosiderophore deoxymugineic acid (Fe-DMA) for growth[12]. To investigate the function of YS1 in iron transport, we tested whether expression of a *ys1* cDNA could restore growth of the *fet3fet4* mutant on medium containing Fe-DMA as the sole iron source. The *ys1* cDNA and the *Arabidopsis* IRT1 cDNA, which encodes an *Arabidopsis thaliana* iron transporter protein capable of supporting growth of the DEY1453 strain on iron citrate[3] were individually transformed into the DEY1453 strain. We then performed a differential growth test using two different sources of iron in the medium, Fe-citrate or Fe-DMA, both at a low concentration (5 μM), to determine the substrate specificity, if any, of YS1 (Fig. 3a, b). Expression of IRT1 restored growth of *fet3fet4* when Fe-citrate was provided as sole iron source, as expected, whereas expression of YS1 did not (Fig. 3a). In the presence of 5 μM Fe-DMA, both YS1 and IRT1 expression allowed growth of *fet3fet4* mutant, possibly owing to small amounts of residual un-chelated Fe(II) present in the medium. To clarify this, the Fe-DMA medium was supplemented with 5 μM 4,7-biphenyl-1,10-phenanthroline-disulphonic acid (BPDS), a strong Fe(II) chelator, to remove any residual Fe(II) from the Fe-DMA medium. Addition of BPDS eliminated complementation by IRT1, without affecting complementation by YS1 (Fig. 3c). The ability of YS1 to allow growth on Fe-DMA in the presence of BPDS strongly suggests that YS1 is a transporter of phytosiderophore-bound Fe(III).

The effect of Fe starvation on *ys1* gene expression was analysed using northern blot hybridization (Fig. 4). Expression of *ys1* was detected in roots of young maize seedlings, as early as 1 day after germination (Fig. 4a, 1+). *ys1* mRNA abundance increased several-fold when plants were grown in absence of iron (Fig. 4a, 1−). The same induction was observed at 5, 7 and 10 days after germination (Fig. 4a, b), showing that steady-state levels of *ys1* mRNA are increased by iron starvation in maize roots. This result agrees well with physiological studies in which maize plants grown under iron-sufficient conditions show a low, basal level of iron uptake, and

a

```
MDLARRGGAAGADDEGEIERHEPAPEDMESDPAAAREKELELERVQSWREQVTLRGVVAA
LLIGFMYSVIVMKIALTTGLVPTLNVSAALMAFLALRGWTRVLERLGVAHRPFTRQENCV
IETCAVACYTIAFGGGFGSTLLGLDKKTYELAGASPANVPGSYKDPGFGWMAGFVAAISF
AGLLSLIPLRKVLVIDYKLTYPSGTATAVLINGFHTKQGDKNARMQVRGFLKYFGLSFVW
SFFQWFYTGGEVCGFVQFPTFGLKAWKQTFFFDFSLTYVGAGMICSHLVNISTLLGAILS
WGILWPLISKQKGEWYPANIPESSMKSLYGYKAFLCIALIMGDGTYHFFKVFGVTVKSLH
QRLSRKRATNRVANGGDEMAALDDLQRDEIFSDGSFPAWAAYAGYAALTVVSAVIIPHMF
RQVKWYYVIVAYVLAPLLGFANSYGTGLTDINMAYNYGKIALFIFAAWAGRDNGVIAGLA
                                    ys1:ref ***
GGTLVKQLVMASADLMHDFKTGHLTMTSPRSLLVAQFIGTAMGCVVAPLTFLLFYNAFDI
                                    ys1:74-1924-1*
GNPTGYWKAPYGLIYRNMAILGVEGFSVLPRHCLALSAGFFAFAFVFSVARDVLPRKYAR
FVPLPMAMAVPFLVGGSFAIDMCVGSLAVFVWEKVNRKEAVFMVPAVASGLICGDGIWTF
                                    ys1-m1::Ac ***
                                        ys1:5344*
PSSILALAKIKPPICMKFTPGS  682
```

b

```
ys1-m1::Ac:
TGCGGTTGCGTCCGGTTAGGGATGAAAA<Ac>CTTTCATCCCTGCGTCCGGTTTGATCTG

ys1:ref:
CGGCAGGGACAACGGCTGTTGGAACCGG<  >GGTTTATTCCTAACAACGGCGTCATCGC
```

c

```
Ys1              CTCACGTTCCTGCTCTTCTACAACGCGTTCGACATCGGGAACCCC
                 L  T  F  L  L  F  Y  N  A  F  D  I  G  N  P …
ys1:74-1924-1    CTCACGTTCCTGCTCTTCTTACAACGCGTTCGACATCGGGAACCC
                 L  T  F  L  L  F  l  q  r  v  r  h  r  e  p …

Ys1              ATGGTGCCTGCGGTTGCGTCCGGTTTGATCTGTGGAGACGGCATA
                 M  V  P  A  V  A  S  G  L  I  C  G  D  G  I …
ys1:5344         ATGGTGCCTGCGGTTGCGTCCGGTGTGCATATGGACC
                 M  V  P  A  V  A  S  G  v  h  m  d …
```

Figure 2 *ys1* sequence analysis. **a**, The predicted amino-acid sequence of YS1. The 12 putative membrane-spanning domains predicted using the SOSUI program are shown boxed[22]. The location of mutations in the *ys1*:ref and *ys1-m1::Ac* are shown below the sequence by asterisks and open asterisks, respectively. **b**, Genomic sequences of the *ys1*:ref and *ys1-m1::Ac* insertion sites. Target site duplications are underlined. **c**, Genomic sequences and predicted translation of non-insertion *ys1* mutations, *ys1:74-1924-1* and *ys1:5344*. Wild-type *Ys1* is shown for comparison.

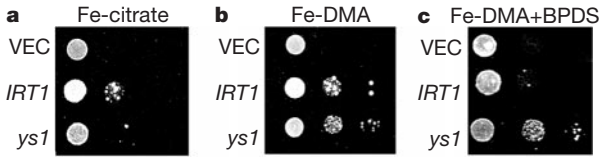

Figure 3 Growth test in the yeast iron uptake mutant. Plasmids expressing IRT1 or YS1 were introduced individually into the DEY1453 strain. The empty pYPGE15 vector was introduced as a control. Yeast growth was on minimal medium/Ura supplemented with 5 μM Fe-citrate (**a**); 5 μM Fe-DMA (**b**); 5 μM Fe-DMA and 5 μM BPDS (**c**). Three yeast cell dilutions were spotted onto the plates.

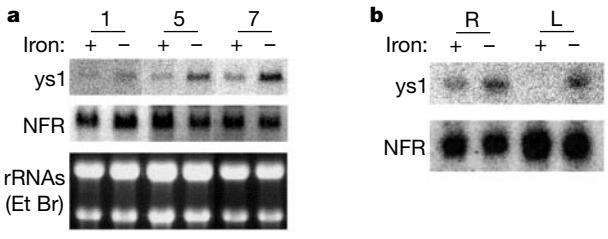

Figure 4 Regulation of *ys1* mRNA levels by iron availability in young maize plantlets. A 3′ UTR *ys1* probe, obtained by PCR, was hybridized to a northern blot containing 10 μg total RNA prepared from either roots (R) or leaves (L). **a**, RNA from roots of 1-, 5-, 7-day-old plantlets; **b**, RNA from roots and shoots of 10-day-old plantlets. The blot was stripped and hybridized to a NADPH-ferric reductase (NRF) cDNA encoding a rice cytochrome b_5 reductase[23] as a loading control. Ethidium-bromide-stained rRNAs are also shown.

show a 2.8-fold increase in the rate of iron uptake in conditions of iron deficiency[8].

Expression of *ys1* in leaves was investigated in 10-day-old plants grown in presence (+) or in absence (−) of iron (Fig. 4b). No *ys1* mRNA was detected in leaves of iron-sufficient plants, but a high level of accumulation was detected in leaves of iron-deficient plants. It is possible that DMA serves as an iron carrier that transports iron from cell to cell inside the plant. Indeed, DMA has been detected in leaves of rice plants[15]. Alternatively, nicotianamine, a Fe(II) and Fe(III) chelator structurally related to DMA[16], might be a substrate for transport by YS1 in tissues other than the root. Nicotianamine is found in all plant species, not just grasses, and has been proposed to be involved in long distance Fe(II) transport in the phloem sap[16–18]. In that regard, we note that the YSL genes of *Arabidopsis*, a species which produces nicotianamine but not mugineic acids, might have a transport role similar to that of YS1. □

Methods

Linkage analysis

The *ys1* locus is located on chromosome 5 of maize, 8 map units distal to the *pr1* locus. Heterozygous *Ys1 pr1 /ys1-m1::Ac Pr1* plants were self-pollinated. Red (*pr1*/*pr1*) and purple (*Pr1*/–) progeny were selected, and their yellow stripe phenotype was observed. The red coloured progeny were predominantly wild type with respect to yellow stripe showing that there is a clear linkage between *ys1-m1::Ac* and *pr1*, as expected. Among the purple progeny, roughly one-third of the individuals were yellow striped, again showing a clear linkage between *ys1-m1::Ac* and *pr1*.

Yeast functional complementation

Three plasmids were individually introduced into the DEY1453 (fet3fet4) strain: the *ys1* cDNA cloned in the expression vector pYPGE15, the *Arabidopsis* IRT1 cDNA cloned in the pFL61 vector[19] (both expressed under the control of the strong PGK promoter[12]) and, as a control, the empty pYPGE15 vector. Minimal medium/Ura was supplemented with 5 μM Fe-citrate, 5 μM Fe-DMA, or 5 μM Fe-DMA and 5 μM BPDS. Three dilutions of the culture (of optical density at 600 nm of 0.2, 0.02, and 0.002) were spotted onto the plates. Growth was carried out for 4 days at 30 °C. The Fe-DMA complex was prepared a described[20].

Plant growth

Plants were grown hydroponically in presence (+) or in absence (−) of iron, for 1, 5, 7 or 10 days after germination, as described[21].

RNA extraction and northern analysis

RNA extraction and RNA blot analysis was performed as described[12]. Hybridization signals were revealed after 3 days exposure, using a PhosphorImager (Storm 480, Molecular Dynamics).

Received 30 May; accepted 31 October 2000.

1. Briat, J. -F. & Lobreaux, S. Iron transport and storage in plants. *Trends Plant Sci.* **2,** 187–193 (1997).
2. Mori, S. Iron acquisition by plants. *Curr. Opin. Plant Biol.* **2,** 250–253 (1999).
3. Eide, D., Broderius, M., Fett, J. & Guerinot, M. L. A novel iron-regulated metal transporter from plants identified by functional expression in yeast. *Proc. Natl Acad. Sci. USA* **93,** 5624–5628 (1996).
4. Yi, Y. & Guerinot, M. L. Genetic evidence that induction of root Fe[III] chelate reductase activity is necessary for iron uptake under iron deficiency. *Plant J.* **10,** 835–844 (1996).
5. Robinson, N. J., Procter, C. M., Connolly, E. L. & Guerinot, M. L. A ferric-chelate reductase for iron uptake from soils. *Nature* **397,** 694–697 (1999).
6. Tagaki, S., Nomoto, K. & Takemoto, T. Physiological aspect of mugineic acid, a possible phytosiderophore of graminaceous plants. *J. Plant Nutr.* **7,** 469–477 (1984).
7. von Wiren, N., Mori, S., Marschner, H. & Romheld, V. Iron inefficiency in maize mutant *ys1* (*Zea mays* L. cv Yellow-Stripe) is caused by a defect in uptake of iron phytosiderophores. *Plant Physiol.* **106,** 71–77 (1994).
8. von Wiren, N., Marchner, H. & Romheld, V. Uptake kinetics of iron-phytosiderophores in two maize genotypes differing in iron efficiency. *Physiol. Plant.* **93,** 611–616 (1995).
9. Hopkins, B. G., Jolley, V. D. & Brown, J. C. Plant utilization of iron solubilized by oat phytosiderophore. *J. Plant Nutr.* **15,** 1599–1612 (1992).
10. Jolley, V. D. & Brown, J. C. Differential response of Fe-efficient corn and Fe-inefficient corn and oat to phytosiderophore released by Fe-efficient Coker 227 oat. *J. Plant Nutr.* **14,** 45–58 (1991).
11. Dellaporta, S. L. & Moreno, M. in *The Maize Handbook* (eds Freeling, M. & Walbot, V.) 219–233 (Springer, New York, 1993).
12. Loulergue, C., Lebrun, M. & Briat, J. F. Expression cloning in Fe^{2+} transport defective yeast of a novel maize MYC transcription factor. *Gene* **225,** 47–57 (1998).
13. Pao, S. S., Paulsen, I. T. & Saier, M. H. Major facilitator superfamily. *Microbiol. Mol. Biol. Rev.* **62,** 1–34 (1998).
14. Stearman, R., Yuan, D. S., Yamaguchi-Iwai, Y., Klausner, R. D. & Dancis, A. A permease–oxidase complex involved in high affinity iron uptake in yeast. *Science* **271,** 1552–1557 (1996).
15. Mori, S. *et al.* Why are young rice plants highly susceptible to iron deficiency? *Plant Soil* **130,** 143–156 (1991).
16. von Wiren, N. *et al.* Nicotianamine chelates both Fe[III] and Fe[II]. Implications for metal transport in plants. *Plant Physiol.* **119,** 1107–1114 (1999).
17. Stephan, U. W., Schmidke, I. & Pich, A. Phloem translocation of Fe, Cu, Mn, and Zn in Ricinus seedlings in relation to the concentrations of nicotianamine, an endogenous chelator of divalent metal-ions, in different seedling parts. *Plant Soil* **165,** 181–188 (1994).
18. Stephan, U. W., Schmidke, I., Stephan, V. W. & Scholz, G. The nicotianamine molecule is made-to-measure for complexation of metal micronutrients in plants. *Biometals* **9,** 84–90 (1996).
19. Minet, M., Dufour, M. E. & Lacroute, F. Complementation of *Saccharomyces cerevisiae* auxotrophic mutants by *Arabidopsis thaliana* cDNAs. *Plant J.* **2,** 417–422 (1992).
20. von Wiren, N., Gibrat, R. & Briat, J.-F. In vitro characterization of iron-phytosiderophore interaction with maize root plasma membranes: evidences for slow association kinetics. *Biochem. Biophys. Acta* **1371,** 143–155 (1998).
21. Thoiron, S., Pascal, N. & Briat, J.-F. Impact of iron deficiency and iron re-supply during the early stages of vegetative development in maize (*Zea mays* L.). *Plant Cell Env.* **20,** 1051–1060 (1997).
22. Hirokawa, T., Boon-Chieng, S. & Mitaku, S. SOSUI: Classification and secondary structure prediction system for membrane proteins. *Bioinformatics* **14,** 378–379 (1998).
23. Bagnaresi, P. *et al.* Cloning and characterization of a maize cytochrome-b_5 reductase with Fe^{3+}-chelate reduction capability. *Biochem. J.* **338,** 499–505 (1999).

Acknowledgements

We are indebted to S. Kawai for the gift of mugineic acid and to M. L. Guerinot for the gift of IRT1 cDNA. This work was supported by a USDA NRICGP Plant Responses to the Environment Award to ELW and an NIH Award to SLD.

Correspondence and requests for materials should be addressed to E.L.W (e-mail: ewalker@bio.umass.edu). The sequence of *ys1* has been deposited at GenBank under the accession number AF186234.

CD45 is a JAK phosphatase and negatively regulates cytokine receptor signalling

Junko Irie-Sasaki*†‡, Takehiko Sasaki*†‡, Wataru Matsumoto§, Anne Opavsky‖, Mary Cheng*, Grant Welstead*, Emily Griffiths*, Connie Krawczyk*, Christopher D. Richardson*, Karen Aitken‖, Norman Iscove¶, Gary Koretzky#, Pauline Johnson☆, Peter Liu‖, David M. Rothstein§ & Josef M. Penninger*‖

* *Amgen Institute, Ontario Cancer Institute, Departments of Medical Biophysics and Immunology, University of Toronto, 620 University Avenue, Toronto, Ontario M5G 2C1, Canada*
§ *Department of Internal Medicine, Yale University School of Medicine, 333 Cedar Street, New Haven, Connecticut 06529-8029, USA*
‖ *Heart and Stroke/Lewar Centre of Excellence in Cariovascular Research, University Health Network, University of Toronto, 200 Elizabeth Street, M5G 2C4, Canada*
¶ *Ontario Cancer Institute, Toronto, Ontario M5G 2M9, Canada*
# *Department of Pathology and Laboratory Medicine, University of Pennsylvania School of Medicine, 421 Cukic Boulevard, Philadelphia, Pennsylvania 19104, USA*
☆ *Departments of Microbiology and Immunology, University of British Columbia, Vancouver, British Columbia V6T 1Z3, Canada*
† *These authors contributed equally to this work*

The regulation of tyrosine phosphorylation and associated signalling through antigen, growth-factor and cytokine receptors is mediated by the reciprocal activities of protein tyrosine kinases and protein tyrosine phosphatases (PTPases)[1]. The transmembrane PTPase CD45 is a key regulator of antigen receptor signalling in T and B cells[2,3]. Src-family kinases have been identified as primary molecular targets for CD45 (ref. 4). However, CD45 is highly expressed in all haematopoietic lineages at all stages of

‡ Present address: Department of Pharmacology, Tokyo Metropolitan Institute of Medical Science, 3-18-22 Honkomagome, Bunkyo-ku, Tokyo, Japan 113-8613.